

Computational and wind tunnel experiment in high-speed ground vehicle aerodynamics

Olexander A. Prykhodko

Dnepropetrovsk National University, 13 Nauchniy Lane, Dnepropetrovsk, 49625, Ukraine

Phone 38 056 370-21-75, e-mail address: paa@mail.dsu.dp.ua

Anatoliy V. Sohatsky, Oleg B. Polevoy, Andrey V. Mendriy

Institute of Transport Systems and Technologies of Ukrainian National Academy of Science, 5 Piesarzhevsky St., Dnepropetrovsk, 49005, Ukraine

ABSTRACT: HSGT aerodynamic characteristics are obtained on the base of numerical simulation and experimental investigation in a wind tunnel. Computational techniques for magnetically levitated transport vehicles are developed on the base of discrete vortex method and Navier-Stokes equations. Aerodynamic analysis of an up-to-date HSGT configuration made it possible to propose the aircraft-type shape for designing the promising magnetically levitated transport vehicles. To improve technical and economical properties of the magnetically levitated transport vehicle trapezoidal arrowhead low-aspect-ratio wing is suggested to use. Investigations showed that lifting properties of the arrowhead wing in the vicinity of track structure are sufficient at low drag.

Keywords: high-speed ground transport vehicle (HSGT), experimental investigation, mathematical simulation, Navier-Stokes equation, aerodynamic characteristics.

INTRODUCTION

Technological and commercial success of the HSGT "MAGLEV" like most of aerospace systems greatly depends on successful aerodynamic configuration. Determination of the aerodynamic loads is a key moment at designing the HSGT, as at high speeds the overall power cost of order from 70% to 90% is necessary to overcome air drag. This in turn significantly influences the determination of linear driver, track structure and controlling equipment characteristics. Besides, it seems to be worthwhile to use aerodynamic forces for increasing the technical and economical performance of MAGLEV transport. One of the ways is to produce the additional lift force using the wing-type configuration of a car.

1 EXPERIMENTAL INVESTIGATION OF HSGT AERODYNAMIC CHARACTERISTICS TYPE FONT, TYPE SIZE AND SPACING

Experiments were conducted in a wind tunnel T-4 of Kharkov Institute of Aviation. To form a configuration of HSGT model preliminary theoretical investigations were carried out with the use of discrete vortex method to evaluate aerodynamics of the transport vehicle. As a result the shape of body, the platform of wing and the type of airfoil were chosen. It was found that thin airfoils with nearly plane CLARK YH-4% type subsurface have optimal characteris-

tics. Calculations showed that it is appropriate to use a trapezoidal platform with an arrowhead leading edge in ground proximity. With the use of results of preliminary calculations HSGT model showed in figure 1 was produced.

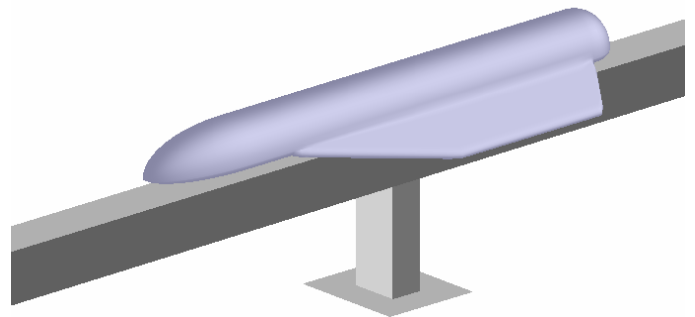


Fig. 1: Conceptual geometry of HSGT MAGLEV "Transmag" produced in the Institute of Transport Systems and Technologies of Ukrainian National Academy of Science

In the field of aviation and space significant aerodynamic experience is stored up based on testing the models in a wind tunnel. Nevertheless the use of experimental methods of simulating the flow around MAGLEV cars involves some difficulties, inherent to this type of vehicles. Here is the case, when we have processes which are difficult to simulate in aerodynamic laboratories.

The main problem is to represent the flow effects, arising when body moves in ground proximity, ade-

quately. In real case in a gap between the ground and a model there should be a gas flow depending on their relative motion. To simulate the ground effect in a wind tunnel one can use the following methods:

1. Stationary plane.
2. Mirror image of model.
3. Boundary layer control.
4. Movable belt.

Figure 2 shows relation between lift coefficient and angle of attack. At negative angle of attack $\alpha = -2^\circ$ the transport vehicle is under effect of negative lift. Increase in angle of attack leads to increase in lift coefficient. At angle of attack $\alpha = 0,4^\circ$ lift becomes zero. At increasing angle of attack there exists linear dependence between lift coefficients of the angle of attack in the range of angles of attack investigated.

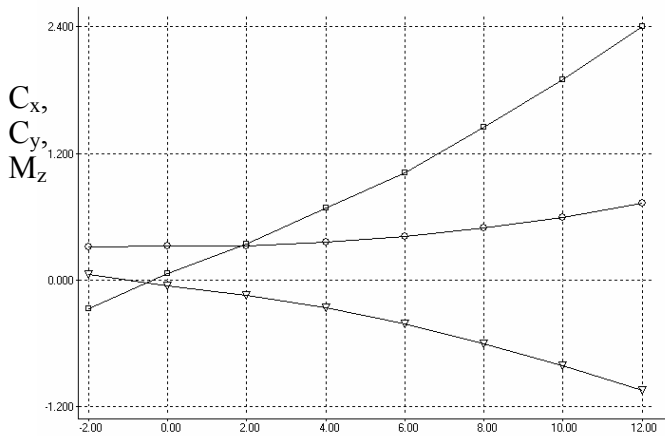


Fig. 2: Relations between drag coefficient ($\circ - C_x$), lift coefficient ($\square - C_y$), pitching moment ($\Delta - M_z$) from angle of attack.

Figure 2 shows drag coefficient dependence of angle of attack, If angle of attack decreases derivative $dC_x/d\alpha$ tends to zero. Increase in angle of attack gives the rise in drag coefficient. In the range of angles from -2° to 2° the rise is not significant but if the angle of attack is more than 2° derivative $dC_x/d\alpha$ grows substantially.

A plot of longitudinal moment coefficient m_z with regard to the leading edge of the winged body against the angle of attack is shown in Figure 3. Longitudinal moment m_z for the range of angles of attack from -2° to -1° is positive, but in the range from -1° to 12° it is negative. Derivative of longitudinal moment coefficient with regard to the angle of attack is negative. That point to the static stability of the model investigated.

Experimental investigation of HSGT aerodynamic performances revealed that winged configuration is worthwhile to use.

Experimental experience suggests that the results are greatly influenced not only by the way of simu-

lating but also by geometrical, kinematical and dynamical performances of units. Analysis shows that no one method for near ground simulating the flow around bodies in a wind tunnel gives possibility to represent the full scale experiment completely.

Besides, physical simulation involves great technical problems and high costs of experiments. Measurement data are in many cases restricted. Such situation appears both at designing and investigating the HSGT, while choosing the optimal configuration, predicting velocity fields in a flow after body, calculating the dynamic performances etc.

To determine the aerodynamics of MAGLEV transport, to understand the mechanisms of flow around bodies a complex approach is required, including both physical experiment and mathematical simulation. Such approach will give possibility to extend the data on velocity, pressure fields and also on integral characteristics, which were received for a model in ground proximity, to a real transport vehicle.

2 METHODS OF NUMERICAL SIMULATION

2.1 Method of discrete vortices

To determine the aerodynamics of HSGT wing the discrete vortex method was applied. In the method Neumann problem for Navier-Stokes equations was reduced to a numerical solution of boundary singular integral equation

$$\frac{1}{4\pi} \frac{\partial}{\partial \bar{n}_{M_0}} \sum_{i=1}^m \int_{\sigma_i} \frac{\partial}{\partial \bar{n}_M} \left(\frac{1}{r_{MM_0}} \right) g_i(M, t) d\sigma_{i,M} = f(M_0, t), \quad (1)$$

where $f(M_0, t)$ – potential function of the double layer, σ_i – vortex surface, $g_i(M, t)$ – potential density of the double layer, m – number of surfaces under consideration. To realize the method a continuous vortex layer is changed into discrete vortex structures. For a wing of finite span attached and free vortex frames are used. Solution of the nonstationary aerodynamic problem for the singular equation system is reduced to the solution of linear algebraic equation system at each time step. Drag distribution over the wing surface is determined using the Cauchy – Lagrange integral.

2.2 Navier–Stokes equations

To obtain discrete analogues with the use of control volume method computational domain is divided into uncrossing cells. Nonstationary compressible gas Navier-Stokes equations are written in the vector integral form:

$$\frac{\partial \mathbf{q}}{\partial t} + \frac{1}{A} \oint_{\Omega} (\mathbf{F} \cdot \bar{\mathbf{n}} - \mathbf{F}_v \cdot \bar{\mathbf{n}}) d\Omega = 0, \quad (2)$$

Here A is cell volume, Ω is surface area, \mathbf{q} is vector of conservative variables, $\bar{\mathbf{F}} \cdot \bar{\mathbf{n}}$ is convective flux vectors and viscous flux vectors $\mathbf{F}_v \cdot \bar{\mathbf{n}}$ in the thin layer approximation have the form

$$\mathbf{q} = \begin{bmatrix} \rho \\ \rho u \\ \rho v \\ \rho w \\ e \end{bmatrix}, \quad \mathbf{F} \cdot \bar{\mathbf{n}} = \begin{bmatrix} \rho U \\ \rho U u + n_x p \\ \rho U v + n_y p \\ \rho U w + n_z p \\ (e + p)U \end{bmatrix},$$

$$\mathbf{F}_v \cdot \bar{\mathbf{n}} = \frac{1}{\text{Re}} \begin{bmatrix} 0 \\ \mu \left(u_n + \frac{1}{3} n_x U_n \right) \\ \mu \left(v_n + \frac{1}{3} n_y U_n \right) \\ \mu \left(w_n + \frac{1}{3} n_z U_n \right) \\ f_{5v} \end{bmatrix}.$$

with

$$f_{5v} = \frac{k}{\text{Pr}(\gamma-1)} (a^2)_n + \frac{\mu}{2} (u^2 + v^2 + w^2)_n + \frac{\mu}{3} U U_n;$$

$$U = n_x u + n_y v + n_z w$$

– velocity in the direction to the external singular normal to the cell surface; n_x, n_y, n_z – single vector components of external normal to the control volume face; $U_n = n_x u_n + n_y v_n + n_z w_n$.

Turbulence model

Mathematical simulation of turbulence remains one of the week fields in the present-day computational fluid dynamics, especially at the background of general progress in numerical methods, computer power, grid generation and flow visualization methods.

The cause/effect mechanism of turbulent instability still remains hypothetical. Turbulent viscosity models, which are based on the empirical data-bases, obtained as a rule for the free shear flows, do not take into account external pressure gradient, surface curvature and other important parameters properly. At the same time approaches based on the large-scale turbulence and direct numerical simulation of turbulence give an extremely high cost of design work.

The applied program package developed includes algebraic, one- and two-parameter models of turbulent viscosity for Reynold-averaged Navier-Stokes equations. Among numerous algebraic closure methods Baldwin-Lomax, Sebetchi-Smith and Soversheny models demonstrate good behavior. Among one-parametric models Glushko-Rubeshin

and Spalart-Allamaras ones should be highlighted. To close Navier-Stokes equations with two additional turbulent transport equations $k-\varepsilon$ model by Johns-Launder and its modification $k-\omega$ model by Menter show high reliability.

Numerical algorithm

To calculate the convective flux vector in (2) the splitting technique is usually used. Flux vectors in the paper are written depending on the normal to the face Mach number $M_n = U/a$. For the supersonic flow in the direction $M_n \geq 1$ we have

$$\hat{\mathbf{F}}^+ = (\mathbf{F} \cdot \bar{\mathbf{n}})^+ = \mathbf{F}, \quad \hat{\mathbf{F}}^- = (\mathbf{F} \cdot \bar{\mathbf{n}})^- = 0, \quad (3)$$

and for the supersonic flow in the backward direction $M_n \leq -1$ we have

$$\hat{\mathbf{F}}^- = (\mathbf{F} \cdot \bar{\mathbf{n}})^- = \mathbf{F}, \quad \hat{\mathbf{F}}^+ = (\mathbf{F} \cdot \bar{\mathbf{n}})^+ = 0. \quad (4)$$

or the subsonic flow $|M_n| < 1$ convective flow are splitted into two components $\hat{\mathbf{F}}^+$ and $\hat{\mathbf{F}}^-$, similarly like Jacobs matrix $\hat{\mathbf{F}}^+$ has positive eigenvalues and Jacobs matrix $\hat{\mathbf{F}}^-$ has negative eigenvalues.

Fluxes are defined using the relations

$$\hat{\mathbf{F}}^\pm = (\mathbf{F} \cdot \bar{\mathbf{n}})^\pm = \begin{bmatrix} f_{\text{mass}}^\pm \\ f_{\text{mass}}^\pm \{ [n_x (-U \pm 2a)/\gamma] + u \} \\ f_{\text{mass}}^\pm \{ [n_y (-U \pm 2a)/\gamma] + v \} \\ f_{\text{mass}}^\pm \{ [n_z (-U \pm 2a)/\gamma] + w \} \\ f_{\text{energy}}^\pm \end{bmatrix} \quad (5)$$

where

$$f_{\text{mass}}^\pm = \pm \rho a (M_n \pm 1)^2 / 4, \quad (6)$$

$$f_{\text{mass}}^\pm = f_{\text{mass}}^\pm \left[\frac{(1-\gamma) U^2 \pm 2(\gamma-1) U a + 2a^2}{\gamma^2 - 1} + \frac{u^2 + v^2 + w^2}{2} \right]. \quad (7)$$

Residual \mathbf{R} is calculated by integration, using the trapezium method of fluxes through each face of the control volume. Residual for convective flux is calculated using the relation

$$\mathbf{R} = - \oint_{\Omega} \mathbf{F} \cdot \bar{\mathbf{n}} d\Omega = - \sum_i \left[\hat{\mathbf{F}}^+(q_i^-) + \hat{\mathbf{F}}^-(q_i^+) \right] \Omega_i \quad (8)$$

Here $\hat{\mathbf{F}}^\pm(q_i^\pm)$ are convective fluxes through the cell faces. To construct the scheme of the first order values of variables are assumed to be constant in the volumes, which are divided by the face. To construct the scheme of higher order variables are extrapolated over the cell surfaces using the special interpolative relation, which give TVD properties to the algorithm.

To obtain an implicit algorithm the equation system (8) is linearized using the splitting of the flux vectors in a Taylor series, then we have

$$[A]^n \{\Delta \mathbf{q}\}^n = \{\mathbf{R}\}^n, \quad (9)$$

$$[A]^n = \frac{S}{\Delta t} \mathbf{I} + \frac{\partial \mathbf{R}^n}{\partial \mathbf{q}} \quad (10)$$

which at each time step are solved using the Gauss-Seidel procedure or conjugated gradients method.

Initial and boundary conditions

On the body surface the conditions of attachment and thermally insulation are set. On the outer boundary undisturbed mainstream parameters are ensured using the Riemann invariants. On other boundaries symmetry and non-reflection or zero-gradient conditions are set depending on a body in consideration.

Realization

Realization of the approach used has been carried out in the framework of the unified package of applied programs. All the stages where numerical methods are extended for the calculation of transport vehicle aerodynamics are realized: choice of the initial statement of a problem; choice of the governing equations; generation of the computational grid; solution of developed numerical algorithm; visualization and analysis of data obtained.

3 NUMERICAL RESULTS

3.1 Calculations with the use of discrete-vortex method

A problem of flow around a wing and an airfoil both in ground proximity and out of its influence has been solved to test the technique realizing the discrete vortex method. In fig. 3 numerical results for the wing in ground proximity are given in comparison with experimental data.

The calculations were carried out for the a flow around the arrowhead wing with a span $\lambda = 2$, leading edge sweep $\chi = 50^\circ$ and construction $\eta = 4$. Fig. 4 gives lift coefficient and pitching moment dependences on angle of attack for a number of distances from a trailing edge of the root chord to the ground. As distance to the ground decreases lift coefficient increases nonlinearly. Analysis of pressure ratios on the wing surface shows that as body approaches the ground redistribution of pressure is taking place on the wing surface. The plot of pressure ratios becomes more complete on the lower part of the wing closer to the lateral trailing edge. It suggests increasing pressure coefficients on these parts of the wing. As a result lift and pitching moment become increased. As angle of attack becomes higher and distance to the ground becomes smaller lift excess decreases due to a separation of the flow from the upper part of the wing. Figure 5 shows drag, lift and pitching moment coefficients against distance to the

ground and angle of attack. Relative thickness of airfoil was chosen to be 0.04 and 0.12. Computational results for aerodynamic coefficients at different angles of attack and distances to the ground are given in Figure 4.

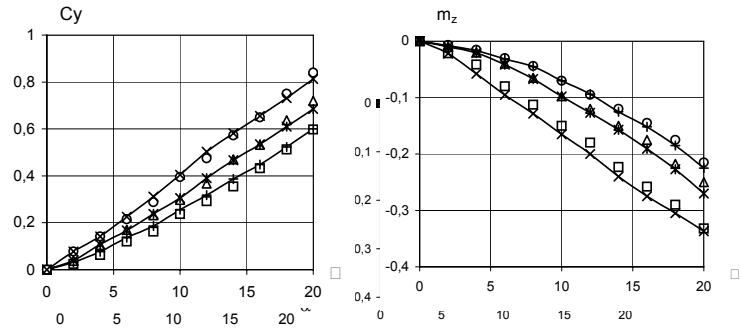


Fig. 3: Relation between airfoil lift coefficient and pitching moment obtained using the discrete-vortex method

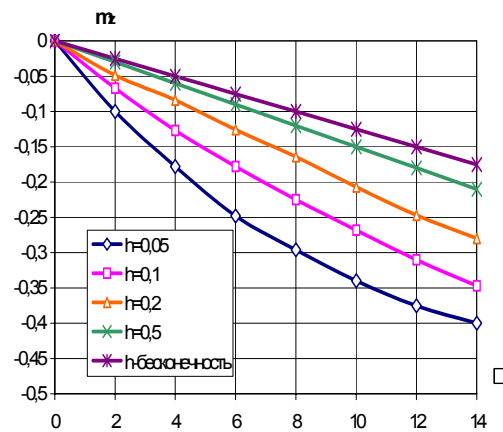
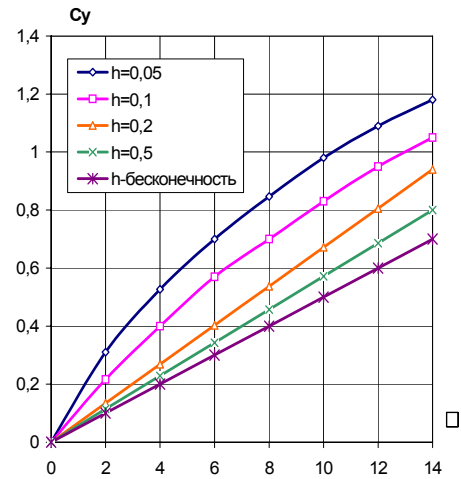


Fig. 4: Plot of lift coefficient and pitching moment for the arrowhead wing $\lambda=2$, $\chi=50^\circ$, $\eta=4$ in ground proximity against angle of attack obtained using the discrete-vortex method

Thus, the calculation gives possibility to make an analysis of a tendency in changing the lift and momentum characteristics for the wing in ground proximity and to chose optimal geometric parameters of the wing to receive its reasonable aerodynamic performance.

3.2 Calculations on the base of Navier-Stokes equations

Numerical investigation of flow around the transport vehicle profile in the vicinity of track structure is carried out. Two configurations of HSGT were chosen for investigation MLU and TRANSMAG. Transport vehicle MLU type was wedge-tailed and wedge-nosed and had a bended bottom to create the effusive diffusive effect. Transmag type vehicle had an aircraft-type configuration with a flat bottom. After solving the Navier-Stokes equations, pressure fields and Cartesian velocity vector components, pressure distribution and distribution of friction coefficients over the profile surfaces of HSGT have been received.

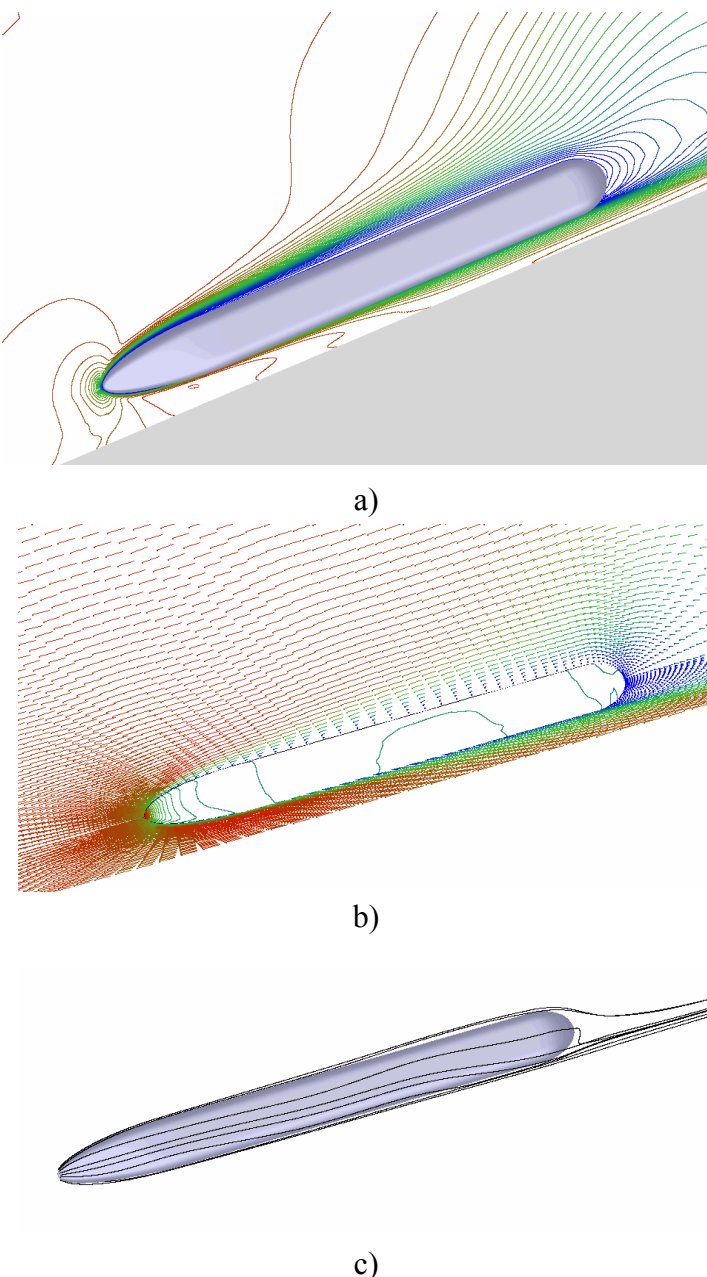


Fig. 5: Distribution of Mach number contours (a), velocity vectors and pressure contours over the surface (b) and spatial streamlines (c) at the unwinged HSGT body in ground proximity

Parametric investigation of a flow structure around two configurations of HSGT is accomplished. The first (unwinged) configuration corresponds to the type of magnetically-levitated transport TRANSRAPID (Germany) and MLU (Japan). The second one is characterized by the presence of finite-span low-aspect-ratio wing and corresponds to the design of the Institute of Transport Systems and Technologies "TRANSMAG".

Wing arrangement has a V-type form with wing inclination -36° . Such shape allows both to reinforce the ground effect and to minimize the losses of aerodynamic quality.

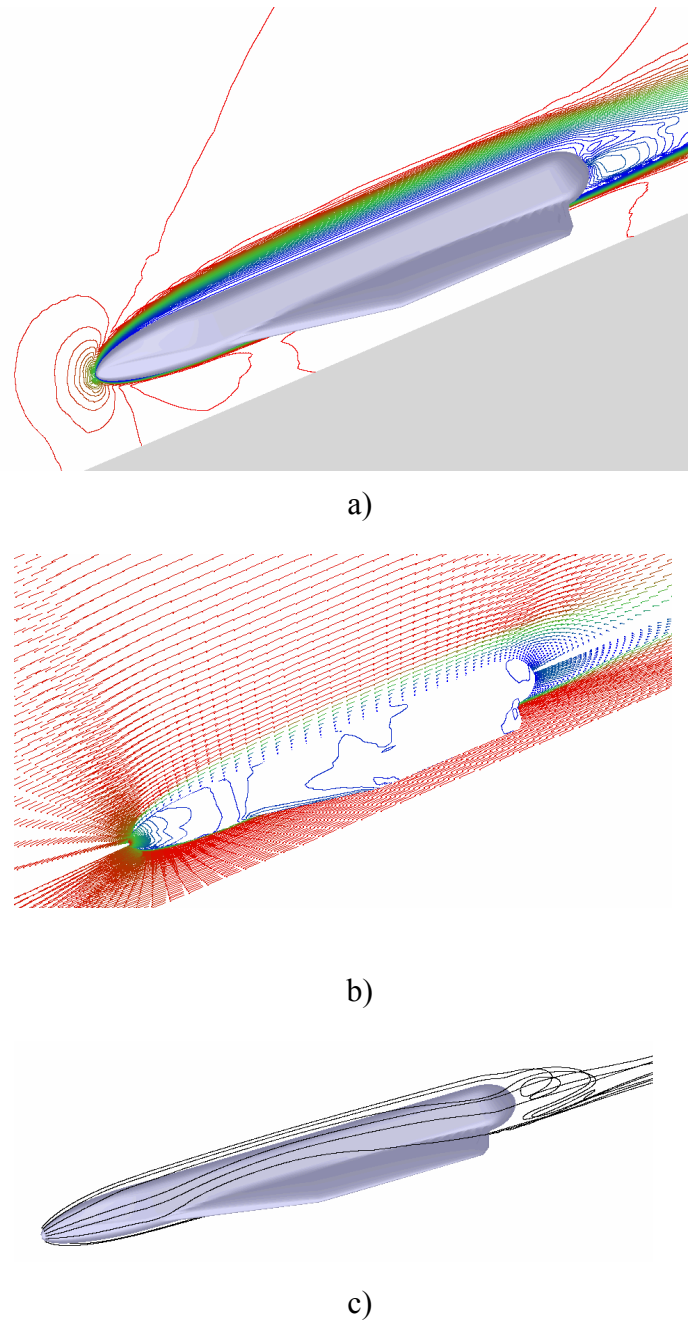


Fig. 6: Distribution of Mach number contours (a), velocity vectors and pressure contours over the surface (b) and spatial streamlines (c) at the winged HSGT body in ground proximity

Calculations are carried out for different aerodynamic gaps $h/L=0.01, 0.1, 0.2, 0.5$ and for the isolated body ($h/L=\infty$). Figures 5, 6 give numerical results at $h/L=0.1$. The overall picture of flow around the HSGT corresponds to the known data on flow around bodies of high aspect ratio (rockets, aircrafts). Mainstream decelerates immediately in front of the body then there occurs the pressure drop on the nose and a “plateau” forms along of the body. In a bottom area (domain) the pressure is somewhat increased due to flow interference. The growth in the boundary layer is taking place along the body and separation occurs in a bottom area.

As the body of HSGT approaches the track structure (aerodynamic gaps h/L decreases) the flow field begins to change. Its outer part remains virtually unchanged but an air stream is forming underneath the bottom with its maximum intensity near the aft part of the body. Such location of the flow peak velocity in the aerodynamic gap is explained by the growth in a boundary layer on a bottom and a track structure, by increasing in the thickness of displacement and accordingly by decreasing in the effective cross section of the aerodynamic gaps.

Overall intensity of the flow in a gaps between the HSGT and a track structure essentially depends on the nose shape. “Lifted” aircraft type configuration assists in catching air mass into the gap (clearance) and in strengthening the air current underneath the bottom resulting in decreasing the pressure on the lower part of the body and in appearing a negative vertical aerodynamic force.

In other words, additional retaining force, counteracting the magnet suspension appears instead lift force. That brings up the need of further investigations to understand how the shapes of nose and aft parts influence aerodynamic characteristics of HSGT.

Including the wing into arrangement of HSGT allows not only to compensate the negative retaining force but to create positive lift force comparable in magnitude with a magnet linear driver.

At the same time the choice of wing profile and its location on the body is an isolated problem. In the configuration considered wings are somewhat displaced to the aft to compensate the unfavorable pitching moment which appears in the case of un-winged type of HSGT. That in turn leads to additional intensification of air current in a gap and to formation of powerful vortex structures in a bottom domain (Figure 6).

CONCLUSIONS

- Computational techniques based on discrete vortex method and Navier-Stokes equations have been developed to calculate aerodynamics of magnetically levitated transport vehicles.
- Algorithms and programs for approximation of HSGT surface and generation of computational grid for HSGT in the vicinity of track structure have been developed.
- Verification and testing of the techniques and algorithms developed have been carried out.
- Analysis of the up-to-date aircraft type HSGT aerodynamic configurations gives possibility to propose to apply the aircraft type configuration at designing the promising magnetically levitated transport vehicles.
- To improve technical and economical parameters of HSGT it is suggested to apply trapezoidal low aspect ratio arrowhead wing. Investigation showed that lifting properties of the arrowhead wing in ground proximity are sufficient at low drag.
- Aerodynamical analysis of winged profiles testifies that CLARK–Y profile families with flat bottom surface and sufficient lifting abilities at low relative thickness have an advantage.

REFERENCES

1. Prykhodko O.A., Polevoy O.B., Mendriy A.V. On the Calculation of Aerodynamic Characteristics of High-Speed Ground Vehicles on the Base of Three-Dimensional Navier-Stokes Equations //Proceedings of 18th International Conference on Magnetically Levitated Systems and Linear Drives. China, Shanghai, 25-29 October 2004.- P. 575-583.
2. Prykhodko O., Sokhatsky A. On the aerodynamic calculation of high-speed ground transport vehicles // 17th international conference on magnetically levitated systems and linear drives. Swiss Federal Institute of technology.- Lausanne, 2002. N PP05201. - 11 pp.